Progress in Natural Science: Materials International 2012;22(3):250–257

Chinese Materials Research Society

Progress in Natural Science: Materials International

www.elsevier.com/locate/pnsmi
www.sciencedirect.com

ORIGINAL RESEARCH

# Preparation and characterization of poly(vinylidene fluoride) composite membranes blended with nano-crystalline cellulose

**Haolong Bai, Xuan Wang, Yitong Zhou, Liping Zhang***

*College of Material Science and Technology, Beijing Forestry University, Beijing 100083, China*

Received 7 March 2012; accepted 12 March 2012
Available online 8 June 2012

**KEYWORDS**

Poly(vinylidene fluoride) (PVDF);
Nano-crystalline cellulose (NCC);
Composite membranes;
Improved performances

**Abstract** Poly(vinylidene fluoride) (PVDF) composite membranes blended with nano-crystalline cellulose (NCC) for ultrafiltration were prepared by a Loeb–Sourirajan (L–S) phase inversion process. The effects of NCC concentration on the membrane performances were investigated. Surface chemical compositions, surface and cross-section morphologies, degree of crystallinity and the thermal stability of the membranes were characterized by Fourier transform infrared spectroscopy (FTIR), scanning electron microscopy (SEM), X-ray diffraction (XRD) and thermal gravimetric analysis (TGA) respectively. The mechanical properties of the membranes were also investigated. All the experimental results indicated that the properties of the composite membranes were improved due to the addition of NCC. The pure water flux of composite membranes can reach 230.8 L/($m^2$ h) and increase up to 47.5% compared with pure PVDF membranes. At the same time, the rejection ratio of a bovine serum albumin solution (1 g/L) was up to 92.5%. The porosity and the mean pore size of the composite membranes were 65% and 49 nm, respectively. Due to the addition of NCC, the degree of crystallinity was increased to 52.1% resulting in the enhanced mechanical properties. A typical asymmetric structure, which was composed of sponge-like dense layer and finger-like microporous support layer, was observed in SEM images of composite membranes.



*Correspondence to: College of Material Science and Technology, Beijing Forestry University, No. 35 Qinghua East Road, Beijing 100083, China. Tel.: +86 13911868160.
E-mail address: zhanglp418@163.com (L. Zhang).



Peer review under responsibility of Chinese Materials Research Society.
http://dx.doi.org/10.1016/j.pnsc.2012.04.011



## 1. Introduction

Ultrafiltration (UF) is a filtration process in which pressure difference is used to act as the driving force. There are many small-sized pores on the surface of ultrafiltration membrane, so ultrafiltation membrane has the capability of holding back macromolecular organic matter, colloid and large-sized particles contained in the stock solution in order to achieve the purposes of separation, concentration and purification.

Due to its advantages such as easy operation, room temperature operation and lower energy consumption, ultrafiltration process has been widely applied in the domain of water treatment, food processing industry and pharmacy

industry, etc [1,2]. For example, ultrafiltration membrane is being employed for water purification in the field of water treatment. Under the action of pressure difference, when tap water flows past the surface of ultrafiltration membrane, colloid, sediment and large-sized particles contained in tap water can be intercepted by ultrafiltration membrane, while water molecules and beneficial minerals can get through the ultrafiltration membrane. As a result, the purified water is obtained.

Poly(vinylidene fluoride) (PVDF) is one of the most widely used UF membrane materials due to its good thermal stability, outstanding chemical and oxidation resistance, highly organic selectivity (It means that PVDF could be dissolved only in some highly polar organic solvents such as N, N-dimethylformamide, N, N-dimethylacetamide and N-methyl-pyrrolidone, etc.) as well as good mechanical property and membrane forming ability [3–7]. However, one of the common problems encountered in the applications of PVDF membranes is membrane fouling. Because of its nature of hydrophobicity, the pure PVDF membranes are apt to be contaminated by proteins and some other impurities in the domain of water and wastewater treatment, which leads to a sharp drop of pure water flux of the membrane [8]. So the permeability of PVDF membrane can be reduced by membrane fouling. The membrane fouling can be eased by membrane cleaning to some extent but it will cost much money. In order to improve the hydrophilicity, permeability and other properties of PVDF membrane, many researches have been carried out, e.g., physical blending, chemical grafting and surface modifying, etc [9,10]. Comparatively speaking, physical blending presents the advantage of an easy preparation by the method of phase inversion [9]. It is well known that nanoparticles have unique magnetic, electronic, mechanical and optical properties to improve the capabilities of polymers in a certain extent because of their small sizes, huge specific surface area and strong activities [11,12]. So blending PVDF with nanoparticles has received much attention. Some inorganic nanoparticals, such as nano $Al_2O_3$ particles [13], nano $TiO_2$ particles [14], etc, have been used to enhance hydrophilicity and other performances of the membrane. However, a potential problem in blending process they may face is particles may not be well dispersed in the polymer solution even at low concentrations.

It is well known that cellulose is an environmental friendly biopolymer and an almost inexhaustible and sustainable polymeric raw material [15]. Nano-crystalline cellulose (NCC) not only retains the characters of natural cellulose such as biodegradability, hydrophilicity and renewability, but also has the features of nanoparticle including huge specific surface area, high mechanical strength and tensile modulus [16,17]. NCC can be generated by chemical or mechanical treatment. The chemical method, such as strong acid hydrolysis, removes the amorphous regions of cellulose fiber and produces nano-size fibrils [18]. The mechanical methods include a high-pressure refiner treatment [19], a high-pressure homogenizer treatment [20], and a grinder treatment [21,22]. Compared with inorganic nanoparticles, NCC with a high axis (L/D) has earned much attention due to its easy availability, low density and renewability [23,24]. In general, cellulose fibrils in nanoscale are very popular for reinforcing polymers and for enhancing hydrophilicity when preparing composite materials [25].

In this study, NCC was prepared by combining with chemical treatment and mechanical treatment. The raw material of nano-crystalline cellulose was cellulose pulp. After the process of acid hydrolysis, the cellulose pulp was homogenized by a high-pressure homogenizer, so that the concentration of the acid during hydrolysis was reduced and the properties of the natural cellulose could be remained. Pure PVDF membranes and NCC/PVDF composite membranes were prepared by a Loeb–Sourirajan (L–S) phase inversion process. The UF properties of prepared membranes were characterized by pure water flux, rejection ratio of a bovine serum albumin solution (1 g/L), porosity and mean pore size. Surface chemical compositions, surface and cross-section morphologies, thermal stability and degree of crystallinity of the membranes were characterized by Fourier transform infrared spectroscopy (FTIR), scanning electron microscopy (SEM), thermal gravimetric analysis (TGA) and X-ray diffraction (XRD) respectively. The mechanical properties of membranes were also measured.

## 2. Experimental

### 2.1. Materials

The poly(vinylidene fluoride) (PVDF) was purchased from Dongguan city special exhibition of plastic raw material Co., Ltd. (Dongguan, China). PEG 4000 and bovine serum albumin (BSA) were purchased from Shantou Xilong Chemical Plant (Shantou, China) and Beijing Aoboxing Biological Technology Co., Ltd. (Beijing, China), respectively. Cellulose pulp was provided by Shandong Huatai Paper Mill (Shandong, China). $H_2SO_4$ (95%–98%), and N, N-dimethylacetamide (DMAc) were purchased from Beijing Chemical Plant (Beijing, China).

### 2.2. Preparation of nano-crystalline cellulose(NCC)

Cellulose pulp was immersed in $H_2SO_4$ (15 wt %) solution and reacted at 85 °C by mixing sufficiently with an electric blender. At the end of the reaction, the pH value of the solution was regulated, using deionized water, until it was neutral. After sieving and drying, the solids were submerged into DMAc and were homogenized with a high-pressure homogenizer (GEA Niro Soavi, Italy) [16]. Subsequently, a colloidal suspension of NCC was obtained. This was then diluted to varying percentages as: 0, 0.05, 0.1, 0.15, 0.2 and 0.25 wt %, in order to check the effects of the NCC on the composite membrane performances.

### 2.3. Preparation of the composite membranes

Composite membranes were prepared by a Loeb–Sourirajan (L–S) phase inversion process. A quantity of PVDF (15 wt %) and PEG 4000 (5 wt %) were dissolved in the prepared NCC colloidal suspension (in different concentrations). The casting solution was obtained by swaying at 60 °C in the table concentrator for 24 h (constant-temperature table concentrator, SHK-99-II, Beijing North TZ-Biotech Develop Co., China). After vacuum degassed (with a vacuum degree of −0.1 MPa.), an appropriate amount of the solution was

dispersed uniformly on a glass plate at ambient atmosphere. After exposed in air for 10 s, the glass plate was immersed into water bath at room temperature. After complete coagulating and washing, the membranes were used for characterization.

### 2.4. Membrane characterization

#### 2.4.1. Fourier transform infrared (FTIR) of the composite membranes

The powders from membrane samples were completely dried at 50 °C in a drying oven before analysis and prepared as KBr pellet. Before being tested by FTIR(Tensor 27, Bruker, Ettlingen, Germany), the KBr pellets were placed on the sample holder and all spectra were recorded in the wave number range of 4000–400 $cm^{-1}$.

#### 2.4.2. Pure water flux and rejection ratio

The pure water flux was tested according to the method described by Zhang et al. [26]. The volume of filtered water $V$ ($m^3$) was obtained in some portions of the membrane with a working pressure of 0.1 MPa and a working time [$t$ (h)]. Next, the pure water flux [$J_w$ (L/($m^2$ h))] was calculated with the following equation:

$$J_w = V/(At) \quad (1)$$

where $V$ is the volume of filtered water ($m^3$), $A$ is the membrane area ($m^2$) and $t$ is the working time (h).

The rejection ratio of the BSA solution (1 g/L) was tested under a working pressure of 0.1 MPa, and the absorbance of the filtered solution was measured at 280 nm with a UV-1801 UV–vi spectrophotometer (Third Analysis Apparatus Co., Shanghai, China) [26]. The rejection ratio was calculated with the following equation:

$$R = (1 - A_f/A_i) \times 100\% \quad (2)$$

where $R$ is the rejection ratio (%) and $A_f$ and $A_i$ are the absorbance of the filtered and initial solutions, respectively.

#### 2.4.3. Porosity and mean pore size

The porosity and mean pore size of the membranes were tested according to the method provided earlier by Zhang et al. [26]. The membrane, having a known area, was weighed in hygroscopic state and then dried in an oven. The porosity [$P_r$ (%)] and mean pore size [$r$ (m)] of the membrane were evaluated with Eqs. (3) and (4).

$$P_r = (W_w - W_d)/(d_w A_m L_m) \quad (3)$$

where $W_w$ is the weight of the wet membrane (g); $W_d$ is the weight of the dry membrane (g); $d_w$ is the water density (g/$cm^3$); and $A_m$ and $L_m$ are the membrane area ($cm^2$) and thickness (cm), respectively.

$$r = [8 \times (2.9 - 1.75P_r) \cdot \eta LF/3600 P_r \Delta P]^{1/2} \quad (4)$$

where $\eta$ is the viscosity of water (Pa s), $L$ is the membrane thickness (m), $F$ is the pure water flux (L/($m^2$ h)), and $\Delta P$ is the working pressure (Pa).

#### 2.4.4. Scanning electron microscopy (SEM)

The composite membranes and pure PVDF membranes were broken in nitrogen liquid, and the fractured cross sections and the bottom surface of the membranes were observed with SEM (S-3000n, Hitachi, Japan) after being sprayed with gold [27].

#### 2.4.5. Mechanical properties

In order to evaluate the mechanical properties of membranes, a tensile testing machine (DCP-KZ300, Sichuan, China) was employed to test the tensile strength and elongation-at-break of membranes. The speed of cross head was 20 mm/min. The dried membranes were snipped into the rectangle shape with width of 15 mm and total length of 100 mm. All of the samples of membranes were tested in ambient condition.

#### 2.4.6. X-ray diffraction (XRD)

The degree of crystallinity of composite membranes was tested with an X-ray diffraction instrument (XRD-6000, Shimadzu, Japan) with Cu Ka radiation, a nickel filter, a wavelength of 0.154 nm, a scan range of $2\theta = 5$–$45°$, and a scan step of $\Delta 2\theta = 0.1°/3$ s.

#### 2.4.7. Thermal gravimetric analysis (TGA)

Thermal stability of membranes was examined by a thermogravimetric analyzer (SHIMADZU, TGA-600, Japan). The experiment was carried out under the $N_2$ atmosphere (20 ml/min). The temperature ranged from 30 to 600 °C with a heating rate of 10 °C/min.

## 3. Results and discussion

### 3.1. Fourier transform infrared (FTIR) analysis

FTIR was employed to investigate the chemical composition of membranes. The FTIR spectrum of NCC was depicted in Fig. 1. As could be seen from Fig. 1, the FTIR absorptions at 3340, 2901, 1430 and 1059 $cm^{-1}$ were related to O–H stretching vibrations of cellulose, C–H stretching vibrations of cellulose, $CH_2$ scissor bending vibration, and C–O stretching vibrations of cellulose, respectively. The peak at 1112 $cm^{-1}$ represented stretching vibration of C–O–C that joins glucose units in the molecule of cellulose. Besides, the absorption at 1632 $cm^{-1}$ was attributed to bending vibration of absorbing H–O–H groups.

The FTIR spectra of the Pure PVDF membranes (a), and Composite membranes (b) were depicted in Fig. 2. The chemical structure of pure PVDF membranes was exhibited in Fig. 2a. The bands located at 3022 and 2980 $cm^{-1}$ corresponded to the

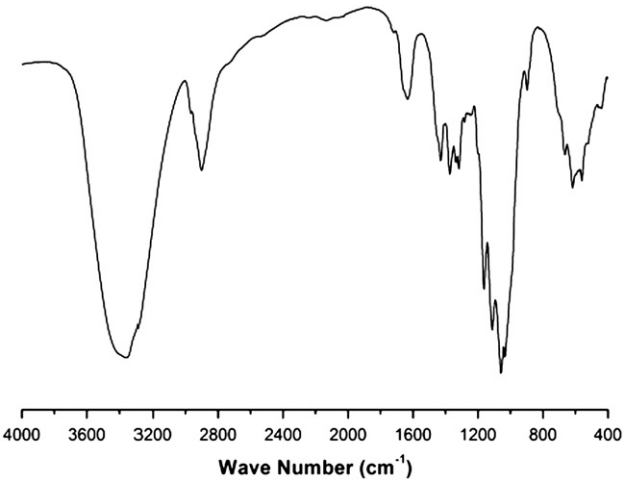


**Fig. 1** FTIR spectrum of the NCC.

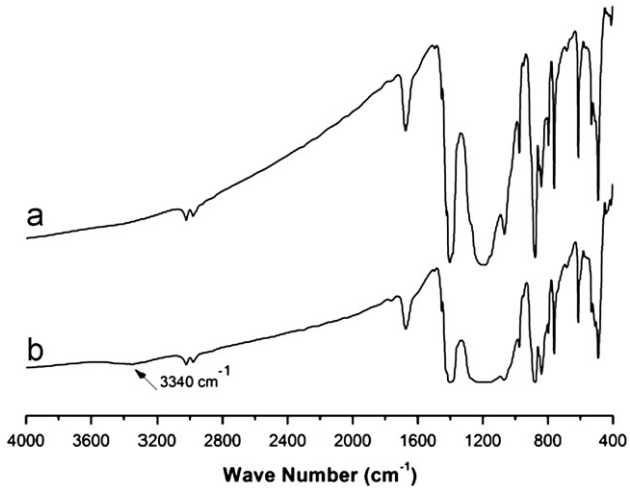


**Fig. 2** FTIR spectrum: (a) Pure PVDF membranes, (b) Composite membranes.

$CH_2$ asymmetric and symmetric vibration of PVDF. The absorption peak appeared at 1403 $cm^{-1}$ was attributed to $CH_2$ wagging vibration. The C–C band of PVDF was observed at 1185 $cm^{-1}$ [28]. The peaks at 878 and 840 $cm^{-1}$ were related to C–C–C asymmetrical stretching vibration and CF stretching vibration of PVDF [29].

The chemical structure of composite membranes was showed in Fig. 2b. It was observed that the characteristic absorption peaks of the pure PVDF membranes were retained by the spectrum of composite membranes (Fig. 2b). For instance, the peaks at 3022 and 2980 $cm^{-1}$ were related to the $CH_2$ asymmetric and symmetric vibration of PVDF. The peak at 1403 $cm^{-1}$ represented $CH_2$ wagging vibration was displayed. The peak at 840 $cm^{-1}$ corresponded to C–F stretching vibration of PVDF was also observed in Fig. 2(b). However, there were differences between Fig. 2(a) and (b). For example, a peak at 3340 $cm^{-1}$ could be observed in Fig. 2(b), while it could not be found in Fig. 2(a). The occurrence of the new absorption peak was attributed to O–H stretching vibration of cellulose. It indicated that the molecule of NCC was existed in the composite membranes. In addition, no other new peaks were observed in the spectrum of composite membranes.

### 3.2. *Pure water flux and rejection ratio*

The data of the pure water flux of different membranes were depicted in Fig. 3. As could be seen from Fig. 3, when the content of NCC ranged from 0 to 0.1 wt %, the pure water flux went up with increasing of NCC contents in the casting solution. This trend may be explained as follows: PVDF belongs to hydrophobic polymer. NCC has good hydrophilic nature. Because it possesses huge specific surface area and it has abundant of hydroxyl groups at its surface. The instantaneous phase separation process could be accelerated due to the addition of NCC to the casting solutions. The permeability of PVDF membranes could be improved by adding certain content of NCC. When the content of NCC was 0.1 wt %, the pure water flux reached a peak value of 230.8 L/($m^2$ h) and increased 47.5% compared with the pure PVDF membranes. When the content of NCC was more than 0.1 wt %, the pure water flux decreased slightly. This was because the phenomenon of agglomeration, which could weaken the permeability of the membranes, could be caused by adding over dose of NCC in the casting solution.

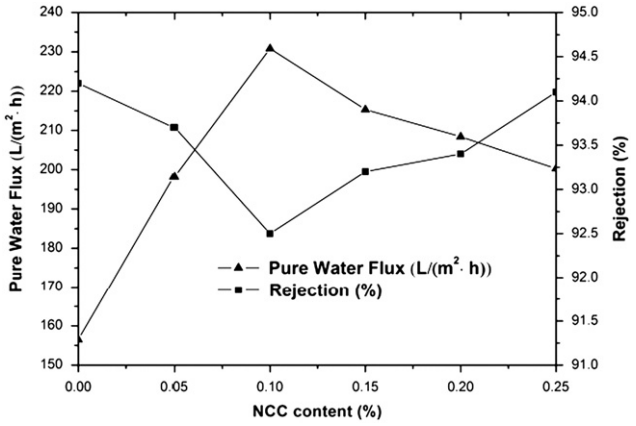


**Fig. 3** Effects of the NCC content on the pure water flux and rejection ratio of the composite membranes.

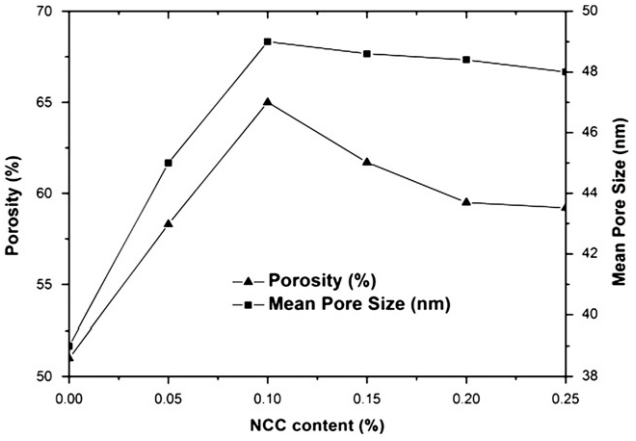


**Fig. 4** Effects of the NCC content on the porosity and mean pore size of the composite membranes.

The BSA rejection ratio results of different membranes were also depicted in Fig. 3. As could be seen from Fig. 3, all of membrane's rejection ratio of BSA could remain at a high level, from 92% to 95%.

### 3.3. *Porosity and mean pore size*

The effects of the nano-crystalline cellulose (NCC) content on the porosity and mean pore size were listed in Fig. 4. Both porosity and mean pore size of membranes were increased with the addition of NCC. The porosity of prepared membranes ranged from 51% to 65%. When the content of NCC was 0.1 wt %, the porosity reached its peak value of 65% and increased 27.5% compared with the pure PVDF membranes. The similar variation trend was also exhibited in the data of the mean pore size with different content of NCC. When the content of NCC was 0.1 wt %, the mean pore size reached its peak value of 49 nm and increased 25.6% compared with the pure PVDF membranes. The difference could be interpreted as follows. NCC was a kind of hydrophilic material. During the

membrane preparation process, the diffusion rate between gels (water) and solvent (DMAc) could be accelerated by NCC. The occurrence of phase separation process, which was good for the generation of polymer-poor phase, was also facilitated by the presence of NCC in membrane preparation process. So the existence of NCC could be beneficial to the formation of membranes with high porosity and mean pore size.

According to the above experimental analysis, a conclusion could be made that 0.1 wt % of NCC in the casting solution was more properly during the process of the preparation of composite membranes.

### 3.4. Morphologies of the membranes

In order to investigate the microstructure of both pure PVDF membranes and composite membranes, SEM images of cross sections and bottom surface of membranes with different compositions had been obtained. A typical asymmetric structure, which was composed of sponge-like dense layer and finger-like microporous support layer, was observed in SEM images of cross section (Fig. 5C and D). In addition, the size of finger-like pore of composite membranes (Fig. 5D) was larger than that of the pure PVDF membranes (Fig. 5C). This was because the process of the pervasion of water getting into the casting solution was accelerated by the presence of NCC. The process of instantaneous phase separation, which provided good condition for the generation of polymer-poor phase, was also speeded up by the existence of NCC and thus structures with large pores were formed. As depicted in Fig. 5, pores were well distributed on the bottom surface of all membranes. Compared with pure PVDF membranes, more pores were exhibited on bottom surface of the composite membranes. This porous structure had a positive effect on improving the pure water flux of composite membranes. According to the above experimental observations, the results indicated that due to the addition of NCC, the composite membranes had a larger size of finger-like pores in cross section and had more pores in the bottom surface.

### 3.5. Mechanical properties

The tensile strength and elongation-at-break of the composite membranes were depicted in Fig. 6. Both of the characterizations were enhanced with adding NCC to the casting solutions. The index of the tensile strength firstly increased with the addition of NCC, attained its peak value when the content of NCC was 0.1 wt % and then decreased in the wake of adding over dose of NCC to the casting solutions. A similar variation trend was observed from the data of the elongation-at-break of composite membranes. The data of the elongation-at-break firstly increased with the addition of NCC, reached its peak value when the content of NCC was 0.1 wt % and then decreased with adding over dose of NCC to the casting solutions. These trends may be explained as follows. The nano effect endowed NCC with lots of characters such as fine mechanical property. Due to its net structure on nanometer scale, NCC had the excellent mechanical property. As a result, the mechanical properties of membranes could be improved by adding appropriate content of NCC. However, the phenomenon of agglomeration, which would weaken the tensile strength and elongation-at-break of the membranes, could be caused by adding excessive amount of NCC in the casting solutions. It was the reason why both of the tensile strength and elongation-at-break decreased when the content of NCC was more than 0.1 wt %. In conclusion, the composite membranes that contained 0.1 wt % NCC had the best mechanical properties. The tensile strength increased from 4.62 MPa of pure PVDF membranes to 6.23 MPa of the

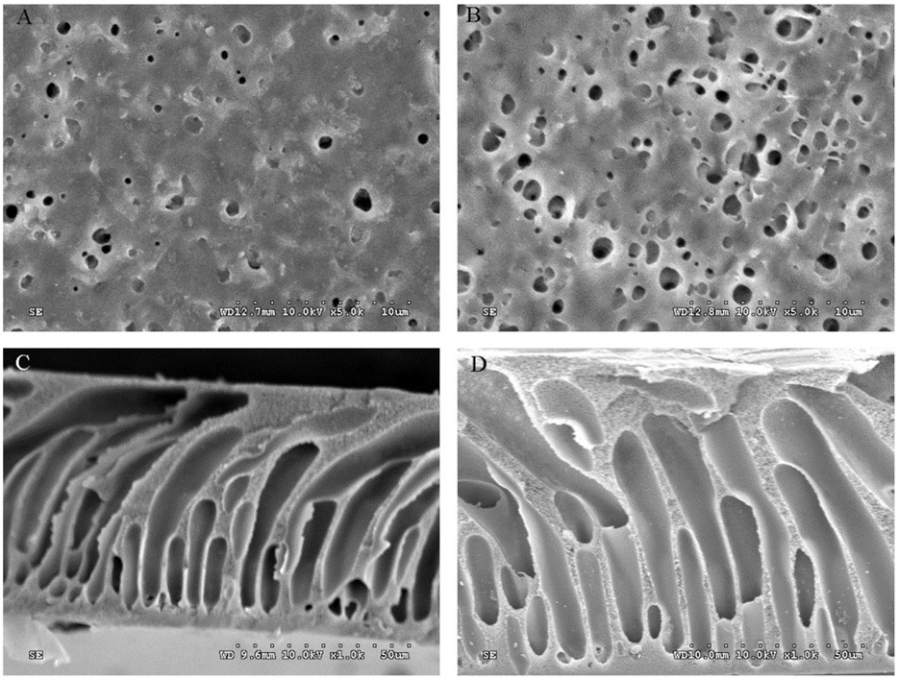


**Fig. 5** SEM images of the pure PVDF membranes and composite membranes. (A) Bottom surface of pure PVDF membranes; (B) bottom surface of composite membranes; (C) cross section of pure PVDF membranes; (D) cross section of composite membranes.

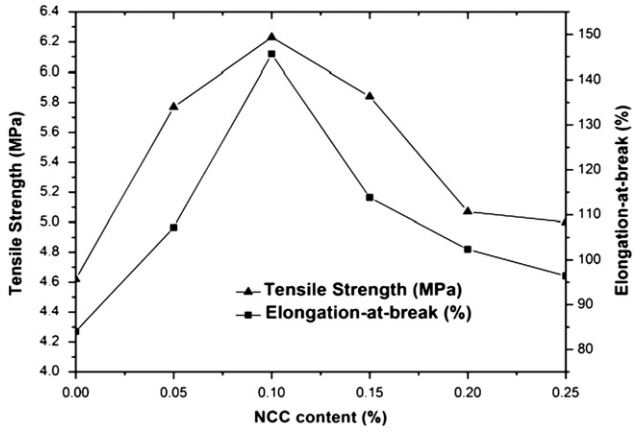


**Fig. 6** Effects of the NCC content on the tensile strength and elongation-at-break of the composite membranes.

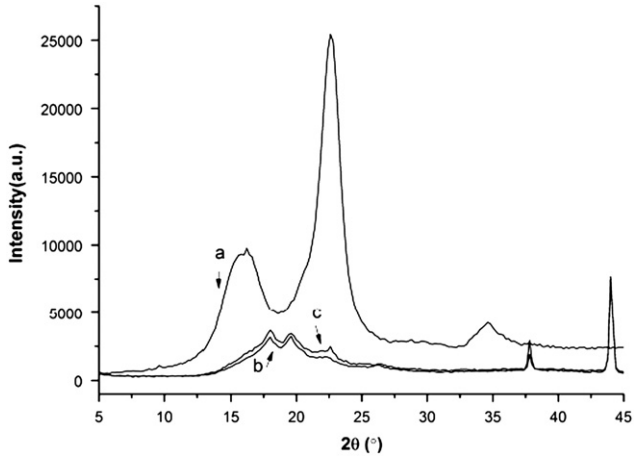


**Fig. 7** X-ray diffraction of NCC (a), pure PVDF membranes (b) and composite membranes (c).

optimal composite membranes. The elongation-at-break of the optimal composite membranes could reach 145.6%, compared with 84.0% of the pure PVDF membranes.

### 3.6. *XRD study*

XRD patterns for NCC, pure PVDF membranes and composite membranes were depicted in Fig. 7 respectively. XRD pattern for NCC was showed in Fig. 7(a). Two obvious characteristic peaks at $2\theta=16.6^\circ$ and $22.6^\circ$ were related to (002) and (001) crystallographic planes, respectively. Both of the two peaks could be attributed to cellulose I, which had a monoclinic structure [2]. The trough appeared at $2\theta=18^\circ$ corresponded to amorphous region of NCC. A weak peak at $2\theta=34.6^\circ$ was attributed to (004) crystallographic plane. The above experimental observations indicated that NCC belonged to semi-crystalline polymer, which contained crystalline regions and amorphous regions. Crystalline form of cellulose I, which had a monoclinic structure, was retained by NCC. The degree of crystallinity of NCC was 59.1% according to calculation by XRD software. In Fig. 7(b), one obvious peak at $2\theta=38.2^\circ$ and three weak peaks at $2\theta=18.2^\circ$, $19.6^\circ$ and $26.4^\circ$ were observed. The peaks at $2\theta=18.2^\circ$, 19.6,

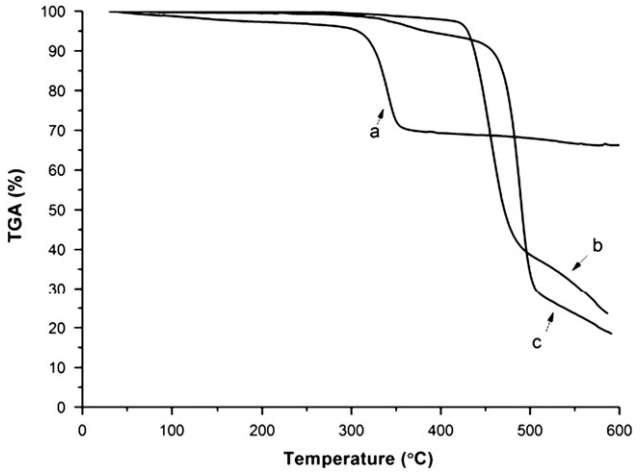


**Fig. 8** TGA Curves of NCC (a), pure PVDF membranes (b) and composite membranes (c).

$26.4^\circ$ and $38.2^\circ$ were related to (020), (100), (021) and (002) crystalline peaks of PVDF $\alpha$ crystalline phase, respectively [30,31]. All of the above characteristic peaks could be observed in the XRD pattern for composite membranes (Fig. 7c), and only the peaks at $2\theta=18.2^\circ$, $38.2^\circ$ became slightly more intensive. A weak peak at $2\theta=22.6^\circ$ could be found in the XRD pattern for composite membranes (Fig. 7c). This characteristic peak was attributed to (001) crystallographic planes of NCC. It indicated that NCC existed in composite membranes. According to calculation by XRD software, the degree of crystallinity of composite membranes was 52.1% and increased by 17.6% compared to that of the pure PVDF membranes. This difference could be attributed to the addition of NCC with high degree of crystallinity.

### 3.7. *TGA analysis*

The thermogravimetric curves of NCC, pure PVDF membranes and composite membranes were displayed in Fig. 8. On account of differences in chemical constitution, NCC and PVDF normally decomposed at different temperature.

Only one weight loss step related to the thermal decomposition of NCC was exhibited by curve a. The weight loss event was observed at 310–340 °C. The weight loss ratio of NCC was 34% at 600 °C. Only one weight loss step ranged from 440 °C to 500 °C was displayed by curve b. This process could be explained as the process of the thermal decomposition of pure PVDF membranes. The weight loss ratio of PVDF was 76.3% at 600 °C. Two weight loss steps were observed in curve c. The first weight loss step observed at 320–360 °C was related to the thermal decomposition of NCC. The second one ranged from 450 to 500 °C was attributed to the thermal decomposition of PVDF. The above experimental observations indicated that the weight loss in composite membranes did not occur until the temperature reached 320 °C.

## 4. Conclusions

Poly(vinylidene fluoride) (PVDF) composite membranes blended with nano-crystalline cellulose (NCC) for ultrafiltration were prepared by a Loeb–Sourirajan (L–S) phase inversion process.

The permeability of the composite membranes was improved by adding NCC. When the content of NCC was 0.1 wt %, the pure water flux of the composite membranes reached 230.8 L/($m^2$ h) and increased 47.5% compared with pure PVDF membranes, and the rejection ratio of a BSA solution (1 g/L) was up to 92.5%. The porosity and the mean pore size of the composite membranes were 65% and 49 nm, respectively. In comparison with the pure PVDF membranes, the porosity and the mean pore size of the composite membranes were increased by 27.5% and 25.6%.

The existence of NCC in the composite membranes was confirmed by the analysis of FTIR. A typical asymmetric structure, which was composed of sponge-like dense layer and finger-like microporous support layer, was observed in the composite membranes images of SEM. Compared with the pure PVDF membranes, the composite membranes had a larger size of finger-like pores in cross section and had more pores in the bottom surface. These observations indicated that the structures of the composite membranes were affected by the addition of NCC.

Both of the tensile strength and elongation-at-break of the composite membranes were enhanced due to the addition of NCC. The crystal structure of cellulose I was retained by NCC according to XRD analysis. The degree of crystallinity of composite membranes was enhanced by adding NCC. A very high thermal stability (the first decomposition temperature was 320 °C) of the composite membranes could be proved by TGA analysis results. Two weight loss steps existed in the TGA curves of composite membranes because of different thermal degradations of PVDF and NCC, respectively.

## Acknowledgment

This research was financially supported by Doctoral Fund of Ministry of Education of China (20110014110012) and Beijing Natural Science Foundation (2112031).

## References

[1] I.C. Kim, J.G. Choi, T.M. Tak, Sulfonated polyethersulfone by heterogeneous method and its membrane performances, Journal of Applied Polymer Science 74 (8) (1999) 2046–2055.
[2] P. Qu, H.W. Tang, Y. Gao, L.P. Zhang, S.Q. Wang, Polyethersulfone composite membrane blended with cellulose fibrils, Bioresources 5 (4) (2010) 2323–2336.
[3] S.S. Chin, K. Chiang, A.G. Fane, The stability of polymeric membranes in a $TiO_2$ photocatalysis process, Journal of Membrane Science 275 (2006) 202–211.
[4] X.C. Cao, J. Ma, X.H. Shi, Z.J. Ren, Effect of $TiO_2$ nanoparticle size on the performance of PVDF membrane, Applied Surface Science 253 (2006) 2003–2010.
[5] J.X. Yang, W.X. Shi, S.L. Yu, Y. Lu, Influence of DOC on fouling of a PVDF ultrafiltration membrane modified by nano-sized alumina, Desalination 239 (2009) 29–37.
[6] L. Yan, S. Hong, M.L. Li, Y.S. Li, Application of the $Al_2O_3$–PVDF nanocomposite tubular ultrafiltration (UF) membrane for oily wastewater treatment and its antifouling research, Separation and Purification Technology 66 (2009) 347–352.
[7] L.Y. Yu, Z.L. Xu, H.M. Shen, H. Yang, Preparation and characterization of PVDF–$SiO_2$ composite hollow fiber UF membrane by sol–gel method, Journal of Membrane Science 337 (2009) 257–265.
[8] K. Jian, P.N. Pintauro, R. Ponangi, Separation of dilute organice/water mixtures with asymmetric poly(vinylidene fluoride) membranes, Journal of Membrane Science 117 (1996) 117–133.
[9] L. Yan, Y.S. Li, C.B. Xiang, Preparation of poly(vinylidene fluoride)(pvdf) ultrafiltration membrane modified by nano-sized alumina ($Al_2O_3$) and its antifouling research, Polymer 46 (2005) 7701–7706.
[10] G.P. Wu, S.Y. Gan, L.Z. Cui, Y.Y. Xu, Preparation and characterization of PES/$TiO_2$ composite membranes, Applied Surface Science 254 (2008) 7080–7086.
[11] Z.P. Fang, Y.Z. Xu, C.W. Xu, Modification mechanism of nanoparticles on polymers, Journal of Material Science and Engineering 21 (2) (2003) 279–282.
[12] P. He, A.C. Zhao, Nanometer composite technology and application in polymer modification, Acromolecule Aviso 2 (2001) 74–82.
[13] F. Liu, M.R. Moghareh Abed, K. Li, Preparation and characterization of poly(vinylidene fluoride) (PVDF) based ultrafiltration membranes using nano $\gamma$-$Al_2O_3$, Journal of Membrane Science 366 (2011) 97–103.
[14] E. Yuliwati, A.F. Ismail, Effect of additives concentration on the surface properties and performance of PVDF ultrafiltration membranes for refinery produced wastewater treatment, Desalination 273 (2011) 226–234.
[15] Dieter Klemm, Dieter Schumann, Friederike Kramer, Nadine HeÔler, Michael Hornung, Hans-Peter Schmauder, Silvia Marsch, Nanocelluloses as Innovative Polymers in Research and Application, Advances in Polymer Science 205 (2006) 49–96.
[16] S. Li, Y. Gao, H.L. Bai, L.P. Zhang, P. Qu, L. Bai, Preperation and characteristics of polysulfone dialysis composite membranes modified with nanocrystalline cellulose, Bioresources 6 (2) (2011) 1670–1680.
[17] M. Henriksson, L.A. Berglund, Structure and properties of cellulose nanocomposite films containing melamine formaldehyde, Journal of Applied Polymer Science 106 (4) (2007) 2817–2824.
[18] S. Beck-Candanedo, M. Roman, D.G. Gray, Effect of reaction conditions on the properties and behavior of wood cellulose nanocrystal suspensions, Biomacromolecules 6 (2) (2005) 1048–1054.
[19] A. Chakraborty, M. Sain, M. Kortschot, Cellulose microfibrils: a novel method of preparation using high shear refining and cryocrushing, Holzforschung 59 (1) (2005) 102–107.
[20] F.W. Herrick, R.L. Casebier, J.K. Hamilton, K.R. Sandberg, Microfibrillated cellulose:morphology and accessibility, Journal of Applied Polymer Science 37 (9) (1983) 797–813.
[21] K. Abe, S. Iwamoto, H. Yano, Obtaining cellulose nanofibers with a uniform width of 15 nm from wood, Biomacromolecules 8 (10) (2007) 3276–3278.
[22] Q.Z. Cheng, S.Q. Wang, T.G. Rials, Poly(vinyl alcohol) nanocomposites reinforced with cellulose fibrils isolated by high intensity ultrasonication, Composite 40 (2009) 218–224 Part A.
[23] J. Lu, P. Askeland, L.T. Drzal, Surface modification of microfibrillated cellulose for epoxy composite applications, Polymer 49 (5) (2008) 1285–1296.
[24] R. Li, J. Fei, Y. Cai, Y. Li, J. Feng, J. Yao, Cellulose whiskers extracted from mulberry: A novel biomass production, Carbohydr, Polymer 76 (1) (2009) 94–99.
[25] J. Ganster, H. Fink, Novel cellulose fibre reinforced thermoplastic materials, Cellulose 13 (3) (2006) 271–280.
[26] L.P. Zhang, G.W. Chen, H.W. Tang, Q.Z. Cheng, S.Q. Wang, Preparation and Characterization of Composite Membranes of Polysulfone and Microcrystalline Cellulose, Journal of Applied Polymer Science 112 (1) (2009) 550–556.
[27] Q.Z. Cheng, S.Q. Wang, T.G. Rials, S.H. Lee, Physical and mechanical properties of polyvinyl alcohol and polypropylene composite materials reinforced with fibril aggregates isolated from regenerated cellulose fibers, Cellulose 14 (2007) 593–602.

[28] A. Rahimpour, S.S. Madaeni, S. Zereshki, Y. Mansourpanah, Preparation and characterization of modified nano-porous PVDF membrane with high antifouling property using UV photo-grafting, Applied Surface Science 255 (2009) 7455–7461.

[29] S. Gu, G.H. He, X.M. Wu, Z.W. Hu, L.L. Wang, G.K. Xiao, L. Peng, Preparation and characterization of poly(vinylidene fluoride)/sulfonated poly(phthalazinone ether sulfone ketone) blends for proton exchange membrane, Journal of Applied Polymer Science 116 (2010) 852–860.

[30] Z.Y. Cui, Y.Y. Xu, L.P. Zhu, J.Y. Wang, B.K. Zhu, Investigation on PVDF-HFP microporous membranes prepared by TIPS process and their application as polymer electrolytes for lithium ion batteries, Ionics 15 (2009) 469–476.

[31] W.Z. Ma, J. Zhang, X.L. Wang, S.M. Wang, Effect of PMMA on crystallization behavior and hydrophilicity of poly(vinylidene fluoride)/poly(methyl methacrylate) blend prepared in semi-dilute solutions, Applied Surface Science 253 (2007) 8377–8388.